Cell. Mol. Life Sci. (2009) 66:3053–3065
DOI 10.1007/s00018-009-0089-0

Cellular and Molecular Life Sciences

RESEARCH ARTICLE

Human mesenchymal stem cells induce E-cadherin degradation in breast carcinoma spheroids by activating ADAM10

Angela Dittmer · Kristina Hohlfeld · Jana Lützkendorf · Lutz P. Müller · Jürgen Dittmer

Received: 4 June 2009 / Revised: 24 June 2009 / Accepted: 25 June 2009 / Published online: 15 July 2009

Abstract Mesenchymal stem cells (MSCs) have been shown to communicate with tumor cells. We analyzed the effect of human MSCs (hMSCs) on breast cancer cells in three-dimensional cultures. By using GFP expression and immunohistochemistry, we show that hMSCs invade 3D breast cancer cell aggregates. hMSCs caused breast cancer spheroids to become disorganized which was accompanied by a disruption of cell–cell adhesion, E-cadherin cleavage, and nuclear translocation of E-cadherin, but not by epithelial/mesenchymal transition or by an increase in ERK1/2 activity. In addition, hMSCs enhanced the motility of breast cancer cells. Inhibition of ADAM10 (a disintegrin and metalloprotease 10), known to cleave E-cadherin, prevented both hMSC-mediated E-cadherin cleavage and enhanced migration. Our data suggest that hMSCs interfere with cell–cell adhesion and enhance migration of breast cancer cells by activating ADAM10.

Keywords MSC · Spheroids · Breast cancer · Migration · ADAM 10 · E-cadherin

Introduction

There is a large body of evidence that the stroma strongly influences tumor progression [1]. Stromal cells, such as fibroblasts, are able to promote tumor cell invasion, e.g., by providing the proteases necessary for the degradation of the extracellular matrix [2]. Endothelial cells are required for the tumor-induced neo-angiogenesis, a critical step in tumor expansion [3]. Lately, stromal mesenchymal stem cells (hMSCs) have also been suggested to contribute to tumor progression. These bone-derived multipotent stem cells are defined by the presence of CD105, CD73, and CD90 and by the lack of typical haematopoietic markers, such as CD45, CD14, or CD35 [4]. hMSCs are also distinct from haematopoietic bone marrow cells in their ability to adhere to plastic surfaces. hMSCs are further characterized by their ability to differentiate into adipocytes, chondrocytes, and osteoblasts [5]. hMSCs are found in many organs and are particularly attracted to injured tissues [6]. hMSCs also enter solid tumors and interact with tumor cells [7–9]. One study showed that hMSCs act on breast cancer cells by secreting the chemokine CCL5 (RANTES) [9]. CCL5 activates its receptor CCR5 on breast cancer cells thereby increasing their metastatic potential. Interestingly, hMSCs are also considered to be a source for carcinoma-associated fibroblasts (CAFs) [10], which are known to promote tumor progression [11]. In addition, by suppressing cancer-fighting immune cells, hMSC may help tumor cells to escape from the host immune surveillance [12]. On the other hand, hMSCs have been demonstrated to also have inhibitory actions on cancer cells [13]. These controversial results may be explained by dose-dependent effects [6].

The ADAM (a disintegrin and metalloprotease) family of metalloproteases are transmembrane or secreted proteins that play a role in the activation of membrane-bound ligands by ectodomain shedding [14]; e.g., pro-mitogens, such as pro-EGF or pro-HB-EGF, have been shown to be substrates of ADAMs which convert these proteins in active ligands that are able to stimulate the EGF receptor.

A. Dittmer · K. Hohlfeld · J. Dittmer (✉)
Klinik für Gynäkologie, Universität Halle,
Halle (Saale), Germany
e-mail: juergen.dittmer@medizin.uni-halle.de

J. Lützkendorf · L. P. Müller
Zentrum für Innere Medizin, Klinik für Innere Medizin IV,
Universität Halle, Halle (Saale), Germany

In addition, ADAMs, in particular ADAM10, control E-cadherin-dependent cell–cell adhesion. Cleavage of the ectodomain of E-cadherin may induce disruption of cell–cell contacts and stimulate the migration of epithelial cells [15].

In the present study, we have analyzed the effect of human hMSCs on human breast cancer cells in three-dimensional (3D) cultures at "low dose" of hMSCs. In 3D cultures, breast cancer cells aggregate to form either tumor spheroids that resemble mammospheres of normal breast epithelial cells [16] or amorphous aggregates [17]. The study revealed that even low numbers of hMSCs disturb the architecture of the spheroids and induce the cleavage of E-cadherin in the tumor cells by an ADAM10-dependent mechanism.

Materials and methods

Cell culture

MDA-MB-231 and MCF-7 cells were maintained in RPMI medium supplemented with 10% fetal calf serum (FCS) in the absence of antibiotics. For 3D cultures, cells were grown as previously described [17]. Briefly, cells were trypsinized and grown on top of a layer of 2% Seakem GTG agarose (dissolved in PBS) without the addition of matrix proteins. The freely floating cells quickly aggregated to form colonies. MCF-7 cell colonies developed into spheroids within 2–3 days, whereas MDA-MB-231 established aggregates of different shapes and sizes. hMSCs were maintained in DMEM (low glucose 1 g/l) supplemented with 10% of the same FCS as used for growing the breast cancer cell lines. hMSCs were kept at low density to avoid differentiation. Co-culturing of breast cancer cells with hMSCs were performed in RPMI/10% FCS. Where indicated, ADAM10 inhibitor GI254023X (kindly provided by GlaxoSmithKline) was added to MCF-7 cells. Real time analysis of hMSCs approaching MCF-7 spheroids were performed by using an AxioCam MRc5 camera and an AxioVision 4 imaging software (Zeiss).

RNA interference

For suppression of ADAM10 or ADAM15 expression, MCF-7 cells were electroporated with ADAM10-, ADAM15-specific, or control si (small interference) RNA following the protocol as described in [17] with some modifications. Briefly, after trypsinization, cells were centrifuged, washed once with RPMI medium (without serum) and resuspended in medium at a density of $\sim$8 million cells per ml. For each transfection, 5 µl siRNA (100 pmol/µl) was added to 250 µl of cell suspension. Electroporation was carried out by using a Bio-Rad GenePulserX-Cell (250 V, 800 µF). Following incubation on ice for 30 min, cells were grown in 75-cm^2 tissue flasks for 2 days, trypsinized and transferred to new flasks for 3D growth. After an additional 2 days, spheroids were collected by centrifugation and plasma membrane extracts were prepared as described below. The sequences of the siADAM10 and siLuc (control siRNA) are as follows. siADAM10 (sense: 5′-UUCUCA CUCUGUAGUAUUAdTdT-3′, antisense: 5′-UAAUACU ACAGAGUGAGGAAdTdT-3′), siLuc (sense: 5′-CUUAC GCUGAGUACUUCGAdTdT-3′, antisense: 5′-UCGAAG UACUCAGCGUAAGdTdT-3′). The sequences of siADAM15 are described in [29].

Isolation and GFP transfection of hMSCs

Human mesenchymal stem cells were isolated from the bone marrow (BM) of patients undergoing diagnostic BM-aspiration after informed consent according to institutional guidelines as described previously [18]. Briefly, mononuclear cells were separated by centrifugation through a Ficoll gradient (PAN), suspended in growth medium and plated at an initial seeding density of 1–2.5 $\times$ 10^5 cells/cm^2. Growth medium was composed of DMEM (low glucose, PAA) supplemented with 15% FCS selected for optimal growth (Invitrogen) and 1% penicillin/streptomycin (PAA). Media were exchanged every 2 days. Cells were passaged after reaching confluence of 50% and replated at 200 cells/cm^2. GFP-expressing MSC were generated by lentiviral transduction. Lentiviral vector particles were produced by transient transfection of HEK 293T cells involving a four-plasmid expression system [19]. The transfer vector plasmid pFUGW [20] carried a GFP gene transcriptionally controlled by the human ubiquitin promoter and a self-inactivating 3′LTR. pMDLg/pRRE and pRSV-Rev were used as packaging plasmids [21]. Vector particles were pseudotyped with vesicular stomatitis virus glycoprotein (VSVG) expressed from pVSVG. All plasmids were kindly provided by Thomas Braun, Max-Planck-Institut für Herz- und Lungenforschung, Bad Nauheim. Briefly, 3.6 $\times$ 10^6 293T cells were plated on 10-cm plates and transfected after 24 h with 10 µg transfer vector plasmid and 5 µg each of packaging and envelope plasmid by calcium phosphate DNA precipitation [22]. After 48 h, the supernatant containing the lentiviral vector was harvested, concentrated by ultracentrifugation, and titered on 293T cells. For transduction, hMSCs were grown to 50% confluence and fed with fresh growth medium containing 8 µg/ml polybrene (Sigma). hMSCs were transduced at passage 1 or 2 with GFP encoding lentiviral vectors at a final concentration of approximately 5 $\times$ 10^5 viral particles/ml. The medium was replaced after 24 h and the transgene expression was analyzed after an additional 24 h.

Western blot analysis

Extraction of cytosolic and nuclear proteins and western blot analysis were performed as described [23]. Plasma membrane proteins were isolated according to Cardone et al. [24] with slight modifications. Briefly, after harvest, cells were resuspended in 400 µl buffer A (10 mM HEPES, pH 7.9, 10 mM KCl, 0.1 mM EDTA, 0.1 mM EGTA and 1 mM DTT) and homogenated by five passes through a G-20 needle, followed by three consecutive centrifugations in a microfuge at 3,000*g* for 10 min to pellet the nuclei, at 6,500*g* for 10 min to clear for mitochondria, lysosomes, peroxisomes and endosomes, and at 13,000*g* for 1 h. The pellet containing plasma membrane proteins was resuspended in buffer C (5 mM HEPES and 0.5 mM EDTA, adjusted to pH 7.2 by KOH, plus 1 mM DTT). The following antibodies were used for western blot analysis: anti-PARP-1 [poly (ADP-ribose) polymerase-1]-25 kD fragment (Epitomics; rabbit monoclonal, 1:10,000), anti-ERK1/2 and anti-phospho-Thr202/Tyr204-ERK1/2 (Cell Signaling Technology; rabbit polyclonal, 1:2,000), anti-CCR5 (Abcam; rabbit polyclonal, 1:1,000), anti-CD44 (Lab vision, mouse monoclonal, HCAM Ab-4, 1:2,000), anti-E-cadherin (BD Transduction Lab.; mouse monoclonal, clone 36, 1:10,000), anti-snail (Abgent; rabbit polyclonal, clone RB1400), anti-ADAM10 (Abcam; ab1997, rabbit polyclonal, 1:1,000 or Calbiochem 422751, rabbit polyclonal, 1:2,000), and anti-vimentin (mouse monoclonal, DAKO, clone V9, 1:1,000). For detection an anti-mouse or anti-rabbit horse radish peroxidase (HRP) conjugate (New England Biolabs) was used.

Immunocytochemistry

Immunocytochemical analysis of formaldehyde fixed and paraffin-embedded 3D cell aggregates were carried out essentially as described [17]. For immunocytochemical staining of adherent cells, cells were grown on Superfrost slides (Menzel) and fixed by formaldehyde. Anti-P-ERK1/2, anti-CD44 and anti-vimentin were used at dilutions of 1:1,000. Anti-PARP-1 (25 kD fragment) and Anti-GFP-HRP (a gift from Miltenyi Biotec) were diluted 1:2,000 and 1:500, respectively.

Migration assays

Cell migration assays (Boyden chamber and wound healing assays) were performed as described [23, 25]. Briefly, cells in the upper compartment of a Boyden chamber were allowed to migrate through an 8-µm pore filter in response to a stimulus produced by cells or to a component of a conditioned medium in the lower compartment. After 1 day cells that remained on the upper side of the filter were wiped off and cells that migrated to the lower side of the filter were fixed, stained with H&E and counted under a microscope (20 fields per filter). For the wound healing assay, a gap was introduced into a monolayer of breast cancer cells in the presence or absence of hMSCs and the wound closure monitored for 2 days. For quantitation, the gap area as visible at 100-fold magnification was measured by using Zeiss Axio Vision R 4.5 software.

Results

hMSCs are attracted by breast cancer cells and invade breast cancer 3D colonies

We have used MCF-7 and MDA-MB-231 breast cancer cells to study the interaction between hMSC and breast cancer cells. E-cadherin-deficient MDA-MB-231 cells have many characteristics of mesenchymal cells and aggregate to irregular structures in 3D culture (Fig. 1g) whereas epithelioid E-cadherin-expressing MCF-7 cells form tumor spheroids (Fig. 1a). MCF-7 spheroids show characteristics of an epithelium with apical tight junctions and desmosomes [26]. Like spheroids derived from immortalized non-tumorigenic MCF-10 breast epithelial cell spheroids [27], MCF-7 spheroids develop a lumen after 7–10 days of culture (Fig. 1b).

To show that lumen formation resulted from apoptosis, sections of formalin-fixed, paraffin-embedded spheroids were analyzed for PARP-1 fragmentation by using an antibody against the 25-kD PARP-1 fragment. PARP-1 specific staining was increased in the center, but not in the periphery, of the spheroids (Fig. 1c, d). PARP-1 fragmentation of MCF-7 cells in 3D was confirmed by western blot analysis (Fig. 1h). Lumen formation was accompanied by a reduced phosphorylation of ERK1/2 (Fig. 1 e, f, h). Phosphorylation of ERK1/2 has been shown to be critical for breast cancer cell survival in 3D culture [17].

Next, we added hMSCs to the MCF-7 spheroids and MDA-MB-231 aggregates in an approximate ratio of 1:1,000. To track hMSCs in breast cancer cell cultures, the hMSCs were retrovirally transfected with a GFP-expression vector (Fig. 2a). Within 1 day of coculturing, fluorescent hMSCs attached to and invaded the 3D colonies of either MCF-7 or MDA-MB-231 cells (Fig. 2b–e). By investigating this process in real time, we found that $\sim$2 h were needed for hMSCs to reach the surface of and enter the spheroid (Fig. 2f).

To confirm that the hMSCs are inside the spheroids, sections of MCF-7 spheroids were immunocytochemically analyzed with a GFP- or a CD44-specific antibody to selectively stain hMSCs. Using immunocytochemical and western blot analysis, we could demonstrate that hMSCs are

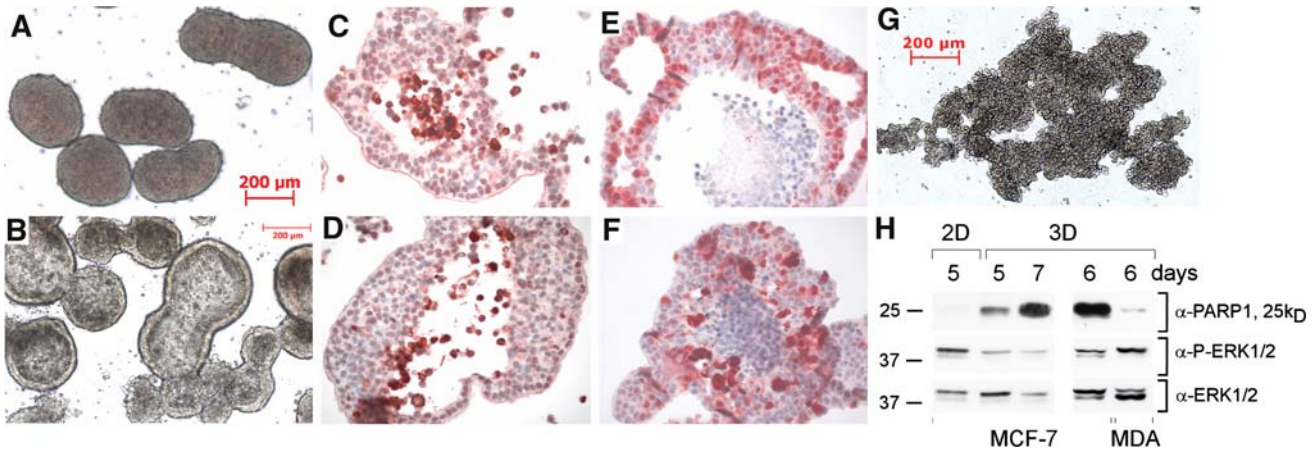

Fig. 1 Homotypic 3D aggregation of MCF-7 and MDA-MB-231 breast cancer cells in 3D. After 3 days in 3D epitheloid MCF-7 cells form spheroids (**a**) that become hollow after additional 4–7 days (**b**). **c–f** Immunohistochemical analyses of sections of paraffin-embedded MCF-7 spheroids. Freely floating cells in the lumen stain positive for the apoptosis marker PARP-1/25 kD fragment (**c**, **d**), but are negative for phosphorylated ERK1/2 (**e**, **f**). Mesenchymal MDA-MB-231 cells form irregular structures in 3D (**g**). **h** Western blot analysis of cytosolic extracts from MCF-7 and MDA-MB-231 cells grown in 2D or 3D. In contrast to MDA-MB-231 cells, MCF-7 cells show strong PARP-1 fragmentation in 3D

positive for CD44 whereas MCF-7 cells are CD44-deficient (Fig. 3a, b, and see Fig. 6a in Section "hMSCs induce degradation of E-cadherin in MCF-7 cells"). In the presence of hMSCs, GFP- and CD44-positive cells could be observed within the spheroids (Fig. 3c–e). By using consecutive sections of MCF-7 spheroids, we were able to show that cells that stained positive for GFP were also positive for CD44 (Fig. 3, compare d with e). Note that more cells immunoreacted to anti-CD44 than to anti-GFP. This is likely to be caused by the stronger reactivity of the anti-CD44 antibody as compared to the anti-GFP antibody. In addition, approximately 40% of the hMSCs showed no or low expression of GFP (Fig. 2a). In the absence of hMSCs, none of the cells in the spheroids reacted to the anti-GFP or anti-CD44 (data not shown). Collectively, these data indicate that hMSCs invaded the MCF-7 cell spheroids.

To show that MCF-7 cells are able to attract hMSCs, we performed migration experiments by using the Boyden chamber technique. MDA-MB-231 or MCF-7 breast cancer cells or conditioned medium from these cells were added to the lower compartment of the Boyden chamber and hMSCs were attached to an 8-µm pore filter in the upper compartment. As a control, we used fresh medium supplemented with serum. When MDA-MB-231 cells or conditioned medium derived from these cells were present in the lower compartment, the number of hMSCs migrating through these pores were enhanced approximately fivefold or threefold, respectively (Fig. 3f). A similar, but weaker, effect (2.5-fold) was observed when MCF-7 cells or conditioned medium from these cells were used. These data suggest that both MDA-MB-231 and MCF-7 cells are able to attract hMSCs by secreting a chemoattractant.

hMSCs disturb tumor spheroid architecture

We next studied the effect of hMSCs on the morphology of breast cancer cell colonies in 3D. MCF-7 spheroids and MDA-MB-231 3D aggregates were incubated with GFP-expressing hMSCs or left untreated. Five days after addition of hMSCs, the MCF-7 spheroids lost their normal morphology and appeared disrupted (Fig. 4a). For further study, spheroids were fixed, paraffin-embedded, cut into sections, immunohistochemically analyzed for CD44 to visualize hMSCs and counterstained with hematoxylin. For this analysis, we chose a 2- instead of 5-day treatment with hMSCs to prevent complete disintegration of the spheroids. The data confirmed that the addition of hMSCs disrupted the normal morphology of the majority of spheroids, causing the smooth ordered edge to become disorganized (Fig. 4, compare b with c). In hollow spheroids that contained hMSCs, both the outside and inside borders turned from very smooth to jagged (Fig. 4c). More importantly, in many hMSC-treated spheroids, the MCF-7 cells were more loosely attached to each other than cells in control spheroids. MDA-MB-231 3D aggregates seemed to be less affected by hMSCs. Nevertheless, MDA-MB-231 3D aggregates often displayed similar changes at their edges as MCF-7 spheroids in response to hMSC treatment (Fig. 4d).

hMSCs increase migration of breast cancer cells

As a consequence of the reduced cell–cell contact as observed in hMSC-treated MCF-7 spheroids, we hypothesized that MCF-7 cells may have a greater potential to migrate. To analyze migration activity, we performed

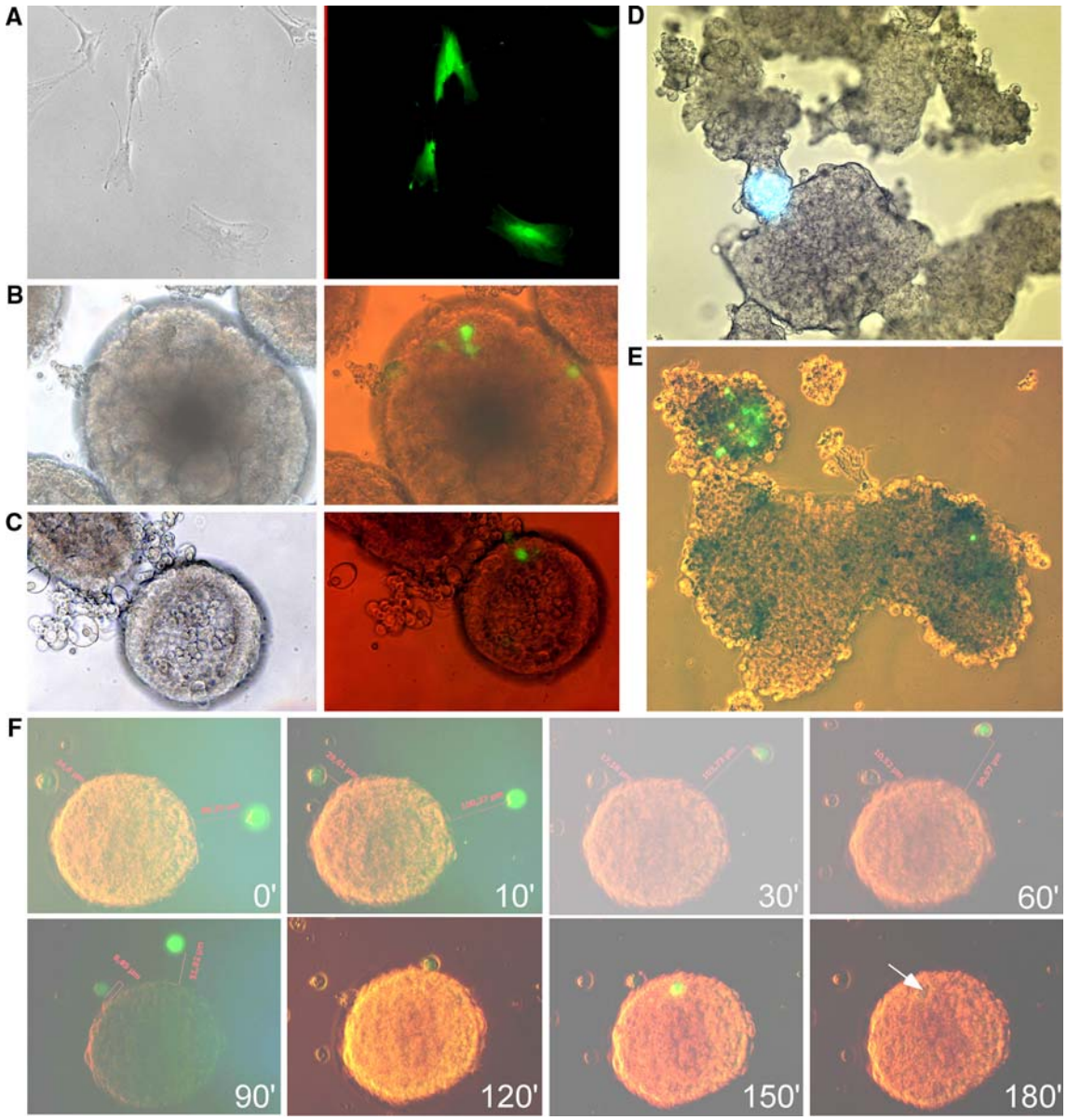

Fig. 2 hMSCs enter MCF-7 and MDA-MB-231 3D colonies. **a** GFP-expressing hMSCs in 2D cultures. **b**, **c** hMSCs entered compact (**b**) and hollow MCF-7 spheroid (**c**) after 1 day of co-culturing. **a**–**c** *Left panel* phase contrast, *right panel* fluorescence. **d**, **e** Incubation of 7-day-old 3D colonies of MDA-MB-231 cells with hMSCs for 2 h (**d**) and for 5 days (**e**). **f** Monitoring of hMSCs approaching and entering a MCF-7 spheroid in real-time

wound healing and Boyden chamber assays. For the wound healing assays, gaps were introduced in MCF-7 monolayers and the closure of these gaps monitored in the presence or absence of hMSCs. We found that, in the presence of hMSCs, the gaps closed much faster than under control conditions (Fig. 5a). To show that hMSCs are present in the wounds, hMSCs were immunocytochemically stained by anti-CD44. In the presence but not absence of hMSCs, large CD44-positive cells were visible within and nearby the gap zone suggesting that hMSCs entered the wound (Fig. 5c). hMSCs may cause MCF-7 cells to migrate faster by secreting a protein that stimulates MCF-7 migration. To test this possibility, we repeated the wound healing assays with conditioned medium (sup) from hMSCs. In the presence of this medium, the migratory activity of MCF-7 cells was also increased (Fig. 5b), whereas no effect could be observed when conditioned medium from MCF-7 cells was used instead. For quantitation, the gap area of the wound was measured. The average gap area under each condition was calculated from the results obtained by three experiments. The data indicate that hMSCs or hMSC supernatants significantly increased MCF-7 migration in the wound healing assay (Fig. 5d). The effect of hMSCs on migration of MCF-7 cells was also analyzed by using a

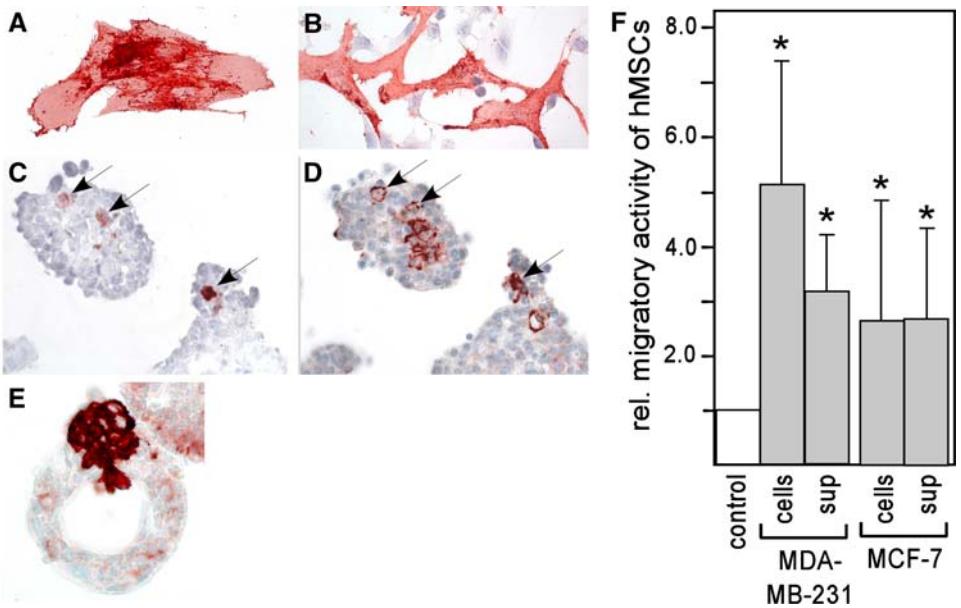

Fig. 3 hMSCs can be detected inside MCF-7 spheroids. **a**, **b** CD44 can be used as a marker to distinguish hMSCs from MCF-7 cells in co-cultures. **a** Cytochemical staining of an adherent hMSC by using a CD44-specific antibody. **b** Cytochemical analysis of a co-culture of adherent hMSCs and MCF-7 cells shows that the larger hMSCs are strongly positive for CD44, whereas the smaller MCF-7 are CD44-negative. **c**–**e** Immunohistochemical analysis of cross-sections of MCF-7 spheroids after incubation with hMSCs. **c**, **d** Consecutive cross-sections analyzed with anti-GFP (**c**) and anti-CD44 (**d**). **e** CD44-positive hMSCs enter a hollow MCF-7 spheroid. **f** Breast cancer cells increase the migratory activity of hMSCs. Migration assays were performed in a Boyden chamber. The upper compartment contained hMSCs attached to an 8-μm pore filter, the lower compartment was filled with medium containing breast cancer cells, cell-free conditioned medium of these cells (sup), or cell-free fresh medium (control). After o/n incubation, hMSCs that migrated through the 8-μm pores were stained and counted. The migratory activity was calculated relative to that under control conditions. *Bars* represent the average value of 3–6 independent experiments, and an *asterisk* indicates that the value is significantly ($P < 0.05$) different to the control value based on a Mann–Whitney *U* test

Boyden chamber. Figure 5e shows that hMSCs enhanced the migratory activity of MCF-7 cells by approximately twofold. We also performed wound healing assays with MDA-MB-231 cells. MDA-MB-231 cells migrated much faster than MCF-7 and closed the gap almost completely within 1 day (data not shown). The addition of hMSCs resulted in a complete closure of the gap within the same period of time, suggesting that hMSCs also affected the migratory activity of MDA-MB-231 cells, but to a much lesser extent. Collectively, these data indicate that hMSCs enhance the migratory activity of breast cancer cells.

hMSCs induce degradation of E-cadherin in MCF-7 cells

Disruption of cell–cell contacts between MCF-7 cells may be caused by E-cadherin degradation. To study this possibility, MCF-7 spheroids were treated with hMSCs or left untreated for 2 days, and E-cadherin expression was monitored in plasma membrane extracts by western blot analysis using an antibody that recognizes the cytoplasmic domain of E-cadherin. Two major proteins, a 120-kD protein representing the full length E-cadherin protein and a 37-kD protein representing a C-terminal fragment (CTF) of E-cadherin [15], could be detected (Fig. 6a). Interestingly, the abundance of CTF increased along with the addition of hMSCs suggesting that hMSCs induced fragmentation of E-cadherin. In addition, the presence of hMSCs caused E-cadherin and a number of anti-E-cadherin reactive proteins with molecular weights ranging from 35 to 55 kD to become more abundant in the nucleus (Fig. 6b). To confirm that E-cadherin in hMSC-treated MCF-7 cells is located in the nucleus, we performed immunohistochemistry. In cells of control spheroids, E-cadherin was mainly found in the periphery of the cells and also in the cytoplasm, but never in the nucleus (Fig. 7, upper panel). In contrast, in spheroids containing hMSCs, E-cadherin was also observed in the nucleus (Fig. 7, lower panel). To stain hMSCs, an antibody against vimentin was used. Vimentin as a marker of mesenchymal cells is strongly expressed in hMSCs, but not in MCF-7 cells (Fig. 6a). It seems that MCF-7 cells that show nuclear E-cadherin are not located in the vicinity of hMSCs. One reason may be that the highly motile hMSCs are moving within the spheroid. As the hMSCs move, they may trigger MCF-7 cells that they meet along their track to translocate E-cadherin to their nuclei. However, by the time the

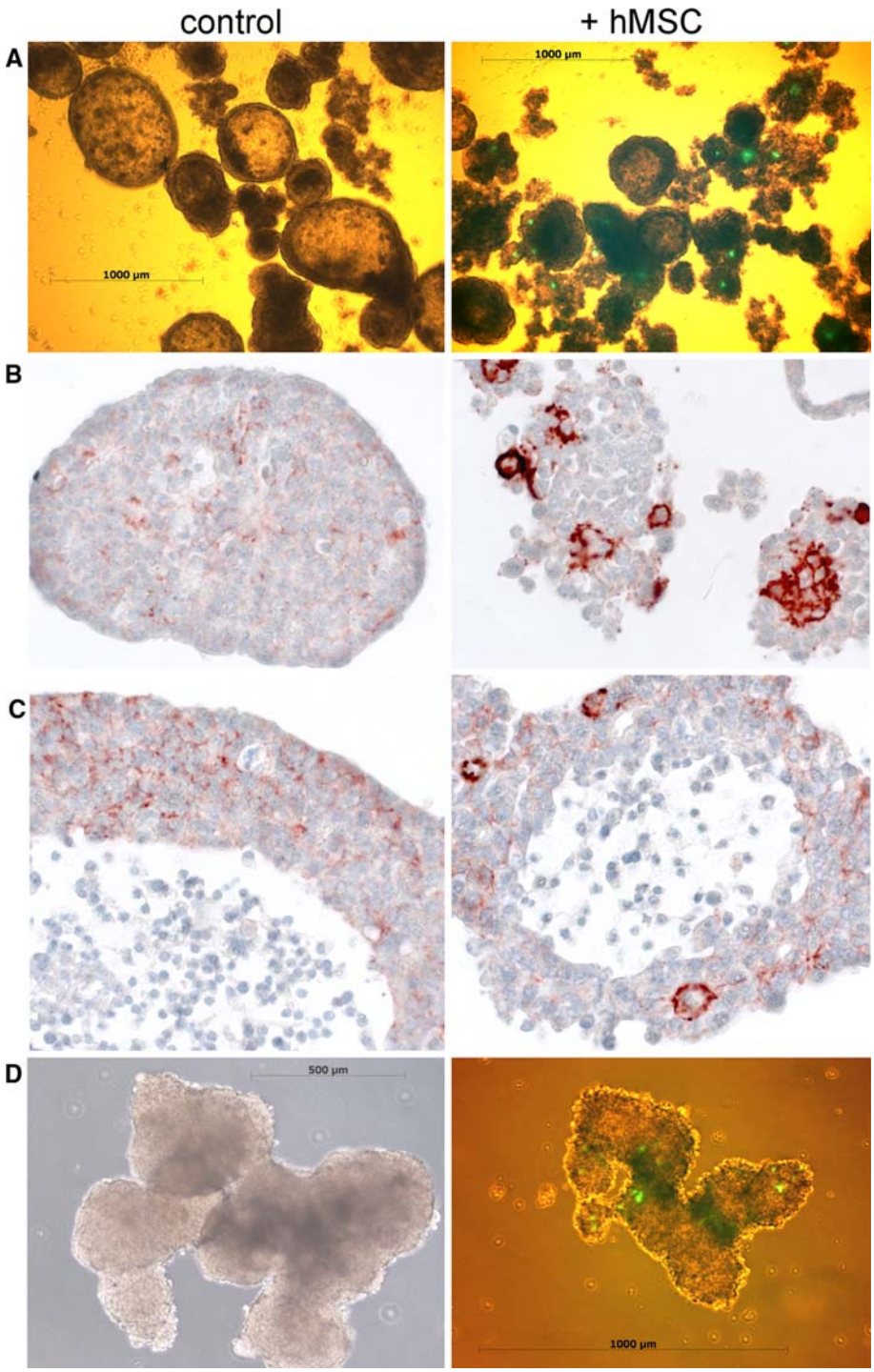

Fig. 4 hMSCs disturb the morphology of the MCF-7 spheroids. **a** Fluorescent/phase contrast microscopy of MCF7 spheroids incubated with and without GFP-expressing hMSCs for 5 days. **b**, **c** MCF-7 spheroids were treated with MSCs or left untreated for 2 days, fixed and paraffin-embedded. Sections were immunohistochemically analyzed by using an antibody against CD44. **d** Fluorescent/phase contrast microscopy of MDA-MB-231 3D aggregates incubated with or without hMSCs for 5 days

E-cadherin enters the nuclei of the target cells, the hMSCs may have moved on and reached a different location.

hMSCs target ADAM10 to induce E-cadherin shedding and migration of MCF-7 cells

A 37-kD CTF has been reported to be generated by E-cadherin cleavage by the sheddase ADAM10 [15]. To study whether ADAM10 may be involved in hMSC-dependent E-cadherin cleavage, we specifically inhibited ADAM10 by the small molecule GI254023X. The presence of this inhibitor strongly reduced the abundance of CTF supporting the notion that ADAM10 was responsible for clipping off CTF from full-length E-cadherin (Fig. 6c). To show that ADAM10 is expressed in MCF-7 cells, the blot was reprobed with an anti-ADAM10 antibody. Two

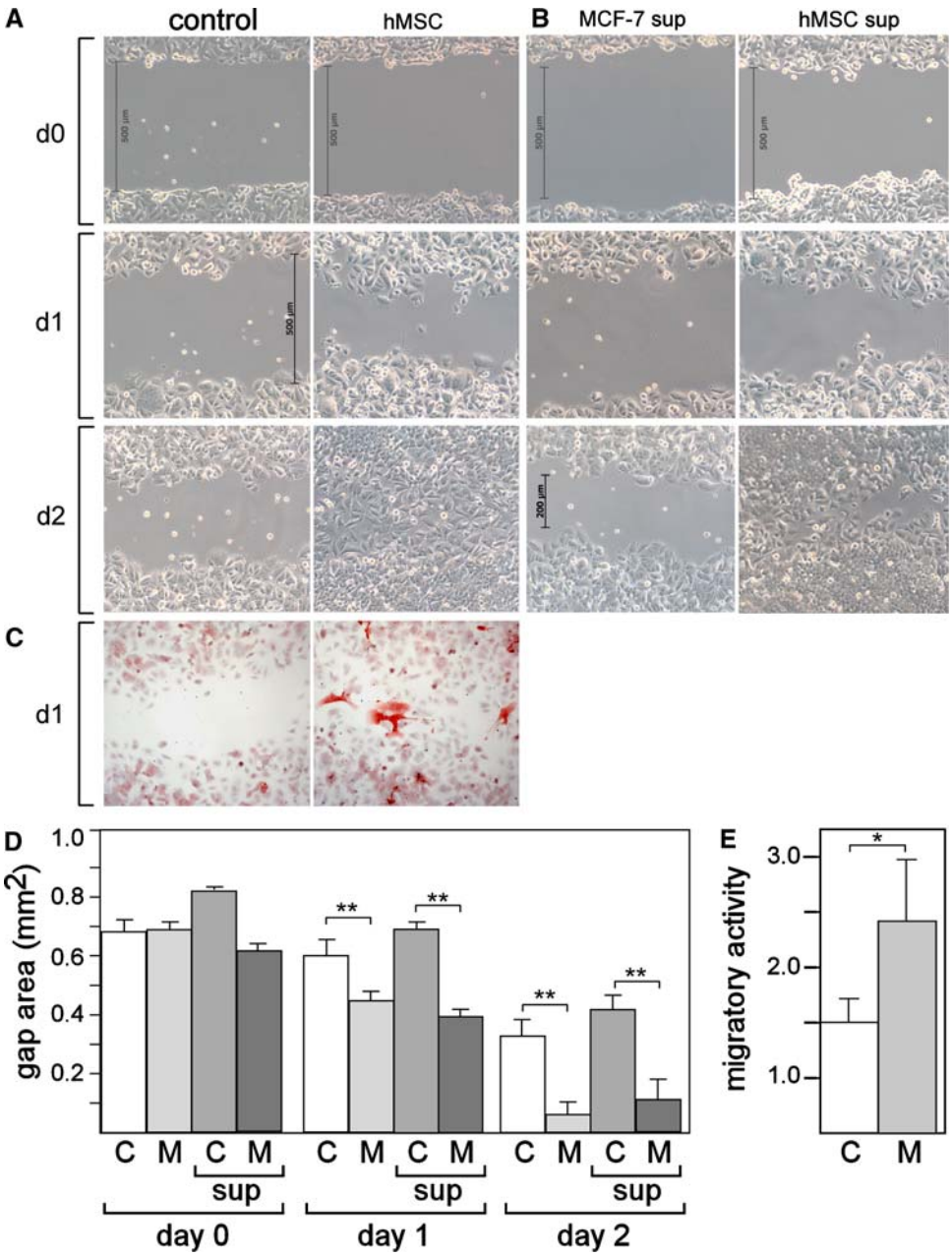

Fig. 5 hMSCs increase migration of breast cancer cells. **a**, **b** Gaps were introduced into monolayers of MCF-7 (**a**) in the presence or absence of hMSCs or (**b**) in the presence of conditioned medium (1 vol + 3 vol fresh medium) from hMSCs (*hMSC sup*) or conditioned medium from MCF-7 cells (*MCF-7 sup*). Closure of the gaps were monitored for 2 days. **c** MCF-7 cells were grown on slides in the presence or absence of hMSCs. One day after the gap was introduced, the cells were fixed and immunocytochemically analyzed for reactivity to an anti-CD44 antibody. **d** Quantitation of results of the wound healing assays shown in (**a**) and (**b**). The gap areas were measured. Each *bar* represent the average area (+SD) of three different wounds at days 0, 1, and 2. **e** Migration assay by using a Boyden chamber. MCF-7 were allowed to migrate through 8-μm pores for 48 h in the absence or presence of hMSCs in the lower compartment. **d**, **e** *C* control, *M* hMSC, *single* or *double asterisks* indicate that values are significantly ($*P < 0.05$ or $**P < 0.002$) different (Student's *t* test)

bands, representing the 100-kD proprotein and a ~70-kD mature protein [28], were visible (Fig. 6c). To confirm that ADAM10 is the major sheddase of E-cadherin in MCF-7 cells, MCF-7 cells were transfected with ADAM10-specific siRNA (siADAM10) and, for comparison, with an siRNA (siADAM15) against ADAM15, another ADAM protein that is able to cleave E-cadherin [14]. As shown in Fig. 6d, siADAM10, but not siADAM15, completely abrogated the appearance of the E-cadherin CTF band in the western blot analysis of plasma membrane extracts. This supports the notion that ADAM10 is responsible for shedding of E-cadherin in MCF-7 cells. Interestingly, we reproducibly found that downregulation of ADAM10 by siADAM10 increased the abundance of ADAM15 in the plasma membrane extract.

ADAMs have also been reported to stimulate migration by activating members of the Her receptor tyrosine kinase family leading to ERK1/2 phosphorylation [14, 29]. Studying the ERK1/2 phosphorylation status, we did not find an increase in ERK1/2 phosphorylation upon treatment of MCF-7 cells with hMSCs (Fig. 6b).

Degradation of E-cadherin is an essential step for epithelial–mesenchymal transition (EMT) [30]. We explored the possibility that hMSCs induce EMT of MCF-7 cells by measuring the expression of the mesenchymal markers vimentin and snail. Both proteins were found to be strongly

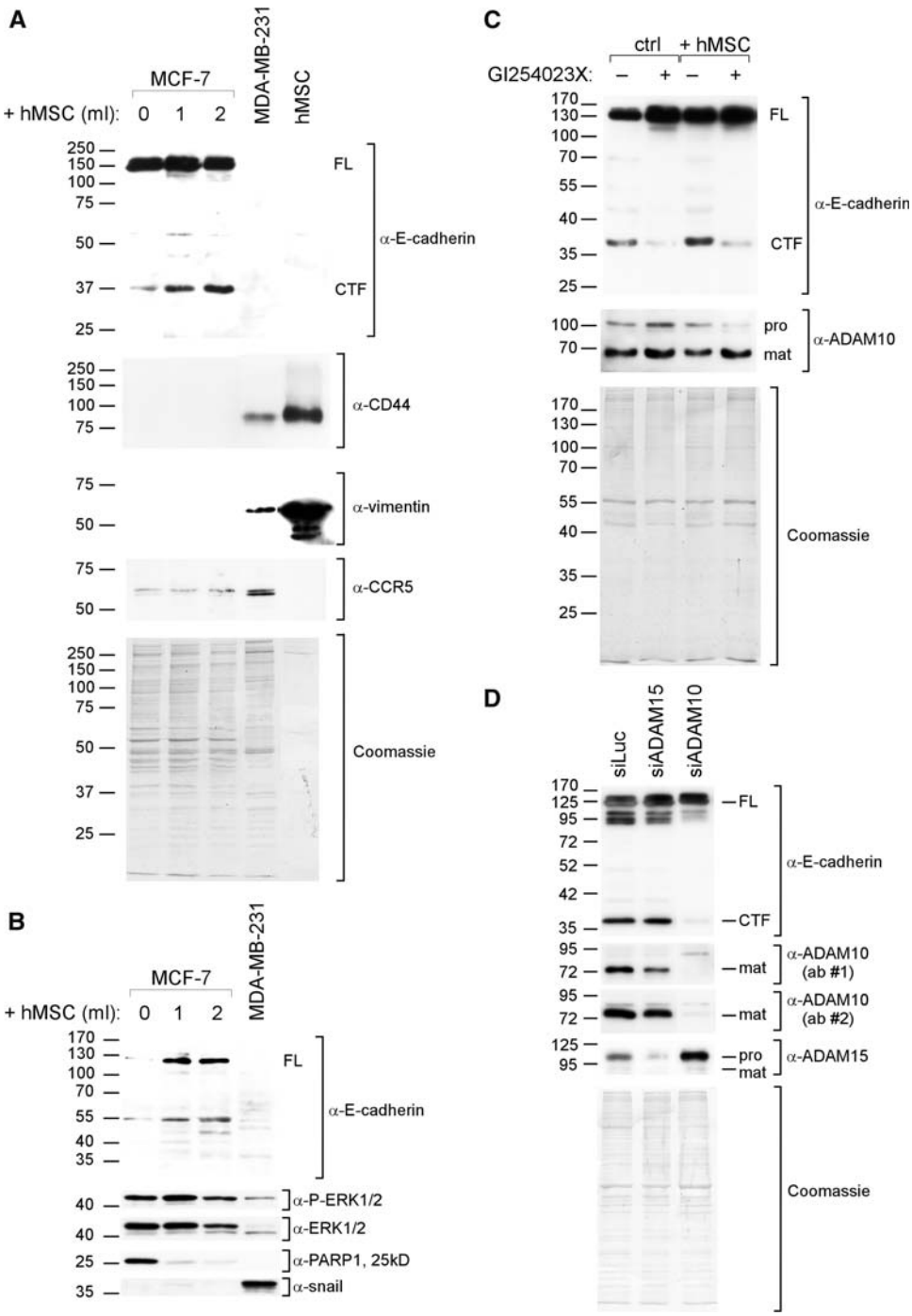

Fig. 6 hMSCs cause E-cadherin in MCF-7 cells to become degraded. **a**–**c** Western blot analyses of plasma membrane (**a**, **c**, **d**) or nuclear extracts (**b**) from MCF-7 cells grown in spheroids in the presence or absence of hMSC (1 and 2 ml equal MCF-7/hMSC ratios of 1,000 and 500, respectively), in the presence or absence of 10 μM ADAM10 inhibitor GI254023X (**c**) or in the presence of ADAM10-specific siRNA (siADAM10), ADAM15-specific siRNA (siADAM15) or control siRNA (siLuc) (**d**). In (**d**) ADAM10 expression was analyzed by two different antibodies (ab #1 and ab #2). For comparison, plasma membrane extracts (**a**) or nuclear extracts (**b**) from 3D-cultured MDA-MB-231 cells and/or hMSCs grown in 2D were run along with MCF-7 extracts. Antibodies used for these analyses are indicated. **a**, **c**, **d** After blotting the protein onto the membrane the proteins remaining in the gel were stained with Coomassie Blue to check for equal loading. In (**b**) ERK1/2 was used as a loading control [38]. *FL* Full length, *CTF* C-terminal fragment, *pro* proprotein, *mat* mature protein

expressed in mesenchymal MDA-MB-231 breast cancer cells, but could not be detected in MCF-7 cells irrespective of whether hMSCs were present or not (Fig. 6a, b). Interestingly, a decrease in PARP-1 fragmentation could be observed in the presence of hMSCs suggesting that hMSCs reduce apoptosis of MCF-7 cells in 3D culture (Fig. 6b).

We next explored the possibility that ADAM10-dependent cleavage of E-cadherin is also responsible for hMSC-accelerated migration. As shown in Fig. 8, 20 μM of the ADAM10 inhibitor GI254023X reversed the effect of hMSCs on MCF-7 cell migration. This suggests that hMSCs causes MCF-7 cells to migrate faster by targeting ADAM10.

Discussion

We show that breast cancer cells attract hMSCs and increase their migratory activity. In turn, hMSCs enter breast cancer spheroids and influence the biology of the

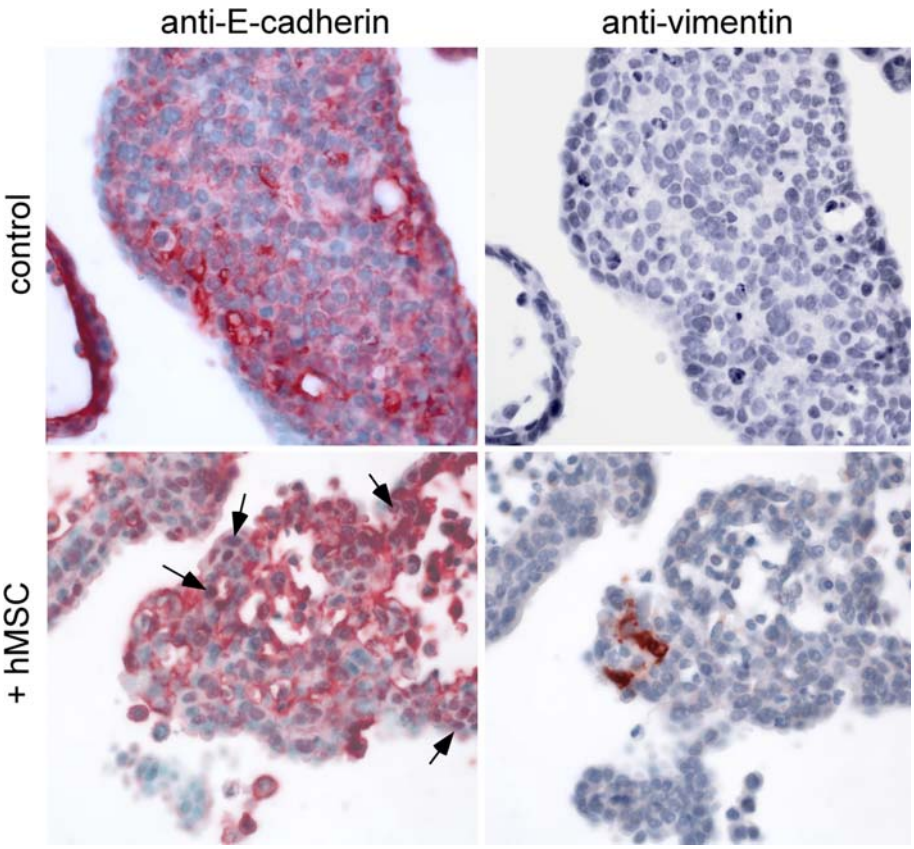

Fig. 7 hMSCs induces transport of E-cadherin to the nucleus in MCF-7 cells. Immunohistochemical analyses of sections of MCF-7 spheroids that were treated with hMSCs or left untreated for 2 days. Consecutive sections of the same spheroid were stained for E-cadherin and for vimentin. *Arrows* indicate examples of reactivity to anti-E-cadherin in the nucleus

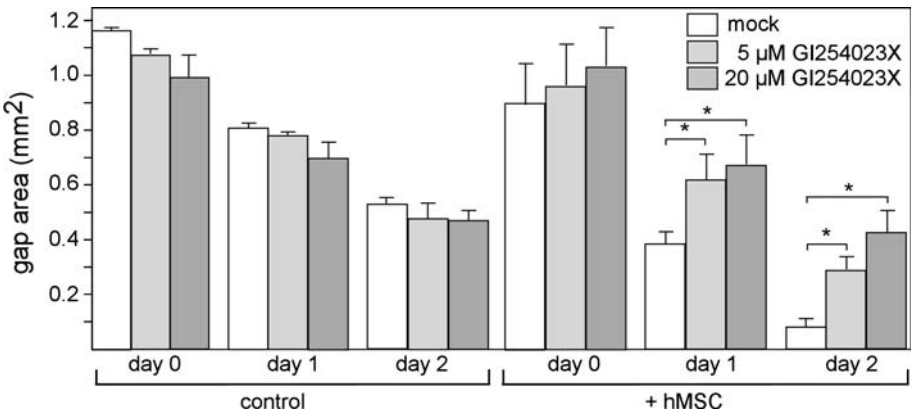

Fig. 8 ADAM10 inhibitor GI254023X inhibits hMSC-dependent migration of MCF-7 cells. Wound healing assays with MCF-7 cells in the presence or absence of hMSCs and/or 20 μM GI254023X. Each *bar* represents the average gap areas (+SD) of 3–6 wounds. *Asterisk* indicates that values are significantly ($P < 0.001$) different (Student's *t* test)

breast cancer cells. The presence of even a few hMSCs altered the morphology of the spheroid and reduced MCF-7 cell–cell adhesion. In addition, the E-cadherin protein was found to be cleaved in response to hMSCs. There is evidence that E-cadherin is the major protein that mediates MCF-7 cell–cell adhesion in spheroids. First, strong E-cadherin-specific staining was observed around the cells of the MCF-7 spheroids (Fig. 7). This observation is consistent with findings reported by dit Faute et al. [26] who also immunohistochemically analyzed MCF-7 spheroids for E-cadherin expression. Second, these authors also showed that the E-cadherin-specific reactivity in MCF-7 spheroids co-localized with desmosomes. Third, electron microscopic analyses of these spheroids confirmed the existence of numerous desmosomes as junctions between cells. It is therefore likely that hMSC-induced shedding of E-cadherin is responsible for the observed reduction in cell–cell contact.

E-cadherin shedding could be prevented by the ADAM10 inhibitor GI254023X or by an ADAM10-specific siRNA, suggesting that E-cadherin shedding in MCF-7 is mainly regulated by ADAM10. Interestingly, GI254023X was also able to prevent hMSCs from enhancing MCF-7 cells migratory activity, suggesting that

hMSC-induced E-cadherin shedding and hMSC-stimulated migration are linked. The migration of the E-cadherin-deficient MDA-MB-231 breast cancer cells was much less affected by hMSCs. The lack of E-cadherin may make these cells less susceptible to hMSCs. Alternatively, their higher intrinsic migratory activity may hide a migration-inducing effect of hMSCs. Our data support a model by which hMSCs enhances migration of breast cancer cells by activating E-cadherin cleaving ADAM10. The importance of ADAM10 in regulating E-cadherin degradation and migration of epithelial cells has also been shown for HaCaT keratinocytes [15]. It has been demonstrated that the large soluble extracellular fragment as generated by ADAM10-dependent cleavage of the E-cadherin disrupts cell–cell adhesion and, thereby, facilitates migration [32].

Extracellular E-cadherin fragments may also stabilize Her2/Her3 heterodimers in MCF-7 cells leading to ERK1/2 activation and subsequent stimulation of migration [29]. Besides E-cadherin cleavage, increased conversion of Pro-EGF to active EGF may also occur upon activation of ADAM10 [14]. By activating its receptor EGFR which is expressed by MCF-7 cells [33], EGF could increase cell migration [34]. EGFR is also involved in E-cadherin internalization which may help to temporarily or permanently disrupt cell–cell adhesion [33]. Activation of the EGFR/Her2/Her3 pathway would lead to an increase in ERK1/2 phosphorylation. However, no increase in ERK1/2 phosphorylation could be observed in response to hMSCs, suggesting that hMSC-activated ADAM10 did not exert its effect on migration through this pathway.

Human mesenchymal stem cells also induced the translocation of E-cadherin into the nucleus. This was shown by western blot analysis as well as by immunohistochemistry. The presence of E-cadherin in the nucleus has been recently documented. Both immunohistochemical studies on certain tumors, such as the pseudopapillary tumor of the pancreas, and cell culture studies have revealed that E-cadherin is translocated to the nucleus [30, 35]. In particular, a 33-kD C-terminal fragment of E-cadherin in conjunction with p120 catenin was found to be transported into the nucleus where it binds to DNA and activates transcription of genes, such as the matrilysin gene [30]. Here, we found that not only C-terminal fragments but also full length E-cadherin were present in the nuclei of hMSC-treated MCF-7 cells. Whether the nuclear E-cadherin proteins play a role in the effect of hMSC on MCF-7 migration is not yet clear. It seems, however, that the ADAM10 inhibitor that completely abrogates hMSC-induced migration of MCF-7 does not prevent, but rather increases, translocation of E-cadherin proteins into the nucleus (data not shown), suggesting that nuclear E-cadherin is not involved in the migration-enhancing effect of hMSCs.

Our data suggest that hMSCs stimulate ADAM10 activity. Not much is known about the mechanism by which ADAMs are activated [14]. Phosphorylation of the cytoplasmic domain and its binding to certain proteins may play a role. The cytoplasmic domain of ADAM10 has been shown to interact with a number of proteins, such as Lck, SAP97, Eve-1, and PACSIN3 [14]. These proteins may be involved in trafficking ADAM10 to the correct cellular location. Correct translocation seems to be required for ADAM10-mediated E-cadherin cleavage in polarized epithelial cells [36]. It has been suggested that Eve-1 and PACSIN3 are activated in response to activated GPCRs [31]. One family of receptors belonging to the superfamily of GPCRs are chemokine receptors. The chemokine CCL5 has been shown to be secreted by hMSCs and to activate migration of MDA-MB-231 cells [9]. However, by using recombinant CCL5, we were unable to demonstrate that CCL5 is responsible for the effect of hMSCs on migration of MCF-7 cells (data not shown), suggesting that other hMSC secretory proteins may be involved that affect E-cadherin-expressing MCF-7 cells. We are currently trying to identify this/these protein(s).

Human mesenchymal stem cells seem to play an important role in wound healing and seem to "mistake" tumors for normal wounds [37]. Attracted by the tumor, hMSCs enter the tumor and secrete certain proteins that may affect tumor growth, tumor progression, and immune response. Most of the data published so far support the notion that hMSCs increase the likelihood of tumor progression, only a few suggest that hMSCs act tumor suppressive [6]. There is some evidence of a dose effect, i.e. that at lower cell number (relative to the number of tumor cells) hMSCs more likely inhibit tumor growth whereas at higher cell number they promote tumor growth. In our study, we used low cell numbers of hMSCs (1:500–1:1,000 relative to the number of breast cancer cells). Despite the low cell number, hMSCs increased migration of the tumor cells. This indicates that only a few hMSCs are necessary to exert a stimulating effect on tumor cells. Our data support the hypothesis that hMSCs are important tumor stromal cells that contribute to tumor progression.

Acknowledgments We thank GlaxoSmithKline for kindly providing us with GI254023X, and Stephan Reshkin for critically reading the manuscript. This work was supported by grant FKZ SI/08 provided by Land Sachsen-Anhalt (Germany).

References

1. Tlsty TD, Coussens LM (2006) Tumor stroma and regulation of cancer development. Annu Rev Pathol 1:119–150
2. Gaggioli C, Hooper S, Hidalgo-Carcedo C, Grosse R, Marshall JF, Harrington K, Sahai E (2007) Fibroblast-led collective invasion of carcinoma cells with differing roles for RhoGTPases in

leading and following cells. Nat Cell Biol 9:1392–400. doi: 10.1038/ncb1658
3. Shchors K, Evan G (2007) Tumor angiogenesis: cause or consequence of cancer? Cancer Res 67:7059–7061
4. Dominici M, Le Blanc K, Mueller I, Slaper-Cortenbach I, Marini F, Krause D, Deans R, Keating A, Prockop D, Horwitz E (2006) Minimal criteria for defining multipotent mesenchymal stromal cells. The International Society for Cellular Therapy position statement. Cytotherapy 8:315–317
5. Pittenger MF, Mackay AM, Beck SC, Jaiswal RK, Douglas R, Mosca JD, Moorman MA, Simonetti DW, Craig S, Marshak DR (1999) Multilineage potential of adult human mesenchymal stem cells. Science 284:143–147
6. Yen L, Yen M-L (2008) Mesenchymal stem cells and cancer—for better or for worse? J Cancer Mol 4:5–9
7. Nakamizo A, Marini F, Amano T, Khan A, Studeny M, Gumin J, Chen J, Hentschel S, Vecil G, Dembinski J, Andreeff M, Lang FF (2005) Human bone marrow-derived mesenchymal stem cells in the treatment of gliomas. Cancer Res 65:3307–3318
8. Studeny M, Marini FC, Champlin RE, Zompetta C, Fidler IJ, Andreeff M (2002) Bone marrow-derived mesenchymal stem cells as vehicles for interferon-beta delivery into tumors. Cancer Res 62:3603–3608
9. Karnoub AE, Dash AB, Vo AP, Sullivan A, Brooks MW, Bell GW, Richardson AL, Polyak K, Tubo R, Weinberg RA (2007) Mesenchymal stem cells within tumour stroma promote breast cancer metastasis. Nature 449:557–563
10. Mishra PJ, Humeniuk R, Medina DJ, Alexe G, Mesirov JP, Ganesan S, Glod JW, Banerjee D (2008) Carcinoma-associated fibroblast-like differentiation of human mesenchymal stem cells. Cancer Res 68:4331–4339
11. Orimo A, Gupta PB, Sgroi DC, Arenzana-Seisdedos F, Delaunay T, Naeem R, Carey VJ, Richardson AL, Weinberg RA (2005) Stromal fibroblasts present in invasive human breast carcinomas promote tumor growth and angiogenesis through elevated SDF-1/CXCL12 secretion. Cell 121:335–348
12. Rasmusson I (2006) Immune modulation by mesenchymal stem cells. Exp Cell Res 312:2169–2179. doi:10.1016/j.yexcr.2006.03.019
13. Khakoo AY, Pati S, Anderson SA, Reid W, Elshal MF, Rovira I, Nguyen AT, Malide D, Combs CA, Hall G, Zhang J, Raffeld M, Rogers TB, Stetler-Stevenson W, Frank JA, Reitz M, Finkel T (2006) Human mesenchymal stem cells exert potent antitumorigenic effects in a model of Kaposi's sarcoma. J Exp Med 203:1235–1247. doi: 10.1084/jem.20051921
14. Edwards DR, Handsley MM, Pennington CJ (2008) The ADAM metalloproteinases. Mol Aspects Med 29:258–289. doi:10.1016/j.mam.2008.08.001
15. Maretzky T, Reiss K, Ludwig A, Buchholz J, Scholz F, Proksch E, de Strooper B, Hartmann D, Saftig P (2005) ADAM10 mediates E-cadherin shedding and regulates epithelial cell–cell adhesion, migration, and beta-catenin translocation. Proc Natl Acad Sci USA 102:9182–9187. doi: 10.1073/pnas.0500918102
16. Dontu G, Abdallah WM, Foley JM, Jackson KW, Clarke MF, Kawamura MJ, Wicha MS (2003) In vitro propagation and transcriptional profiling of human mammary stem/progenitor cells. Genes Dev 17:1253–1270
17. Dittmer A, Schunke D, Dittmer J (2008) PTHrP promotes homotypic aggregation of breast cancer cells in three-dimensional cultures. Cancer Lett 260:56–61. doi:10.1016/j.canlet.2007.10.020
18. Mueller LP, Luetzkendorf J, Mueller T, Reichelt K, Simon H, Schmoll HJ (2006) Presence of mesenchymal stem cells in human bone marrow after exposure to chemotherapy: evidence of resistance to apoptosis induction. Stem Cells 24:2753–2765. doi:10.1634/stemcells.2006-0108
19. Mochizuki H, Schwartz JP, Tanaka K, Brady RO, Reiser J (1998) High-titer human immunodeficiency virus type 1-based vector systems for gene delivery into nondividing cells. J Virol 72:8873–8883
20. Lois C, Hong EJ, Pease S, Brown EJ, Baltimore D (2002) Germline transmission and tissue-specific expression of transgenes delivered by lentiviral vectors. Science 295:868–872. doi:10.1126/science.1067081
21. Dull T, Zufferey R, Kelly M, Mandel RJ, Nguyen M, Trono D, Naldini L (1998) A third-generation lentivirus vector with a conditional packaging system. J Virol 72:8463–8471
22. Chen C, Okayama H (1987) High-efficiency transformation of mammalian cells by plasmid DNA. Mol Cell Biol 7:2745–2752
23. Dittmer A, Vetter M, Schunke D, Span PN, Sweep F, Thomssen C, Dittmer J (2006) Parathyroid hormone-related protein regulates tumor-relevant genes in breast cancer cells. J Biol Chem 281:14563–14572. doi:10.1074/jbc.M510527200
24. Cardone RA, Bellizzi A, Busco G, Weinman EJ, Dell'Aquila ME, Casavola V, Azzariti A, Mangia A, Paradiso A, Reshkin SJ (2007) The NHERF1 PDZ2 domain regulates PKA-RhoA-p38-mediated NHE1 activation and invasion in breast tumor cells. Mol Biol Cell 18:1768–1780. doi:10.1091/mbc.E06-07-0617
25. Schunke D, Span P, Ronneburg H, Dittmer A, Vetter M, Holzhausen HJ, Kantelhardt E, Krenkel S, Muller V, Sweep FC, Thomssen C, Dittmer J (2007) Cyclooxygenase-2 is a target gene of rho GDP dissociation inhibitor beta in breast cancer cells. Cancer Res 67:10694–10702
26. dit Faute MA, Laurent L, Ploton D, Poupon MF, Jardillier JC, Bobichon H (2002) Distinctive alterations of invasiveness, drug resistance and cell–cell organization in 3D-cultures of MCF-7, a human breast cancer cell line, and its multidrug resistant variant. Clin Exp Metastasis 19:161–168
27. Muthuswamy SK, Li D, Lelievre S, Bissell MJ, Brugge JS (2001) ErbB2, but not ErbB1, reinitiates proliferation and induces luminal repopulation in epithelial acini. Nat Cell Biol 3:785–792
28. Hakulinen J, Keski-Oja J (2006) ADAM10-mediated release of complement membrane cofactor protein during apoptosis of epithelial cells. J Biol Chem 281:21369–21376. doi:10.1074/jbc.M602053200
29. Najy AJ, Day KC, Day ML (2008) The ectodomain shedding of E-cadherin by ADAM15 supports ErbB receptor activation. J Biol Chem 283:18393–18401. doi:10.1074/jbc.M801329200
30. Ferber EC, Kajita M, Wadlow A, Tobiansky L, Niessen C, Ariga H, Daniel J, Fujita Y (2008) A role for the cleaved cytoplasmic domain of E-cadherin in the nucleus. J Biol Chem 283:12691–12700. doi:10.1074/jbc.M708887200
31. Ohtsu H, Dempsey PJ, Eguchi S (2006) ADAMs as mediators of EGF receptor transactivation by G protein-coupled receptors. Am J Physiol Cell Physiol 291:C1–C10
32. Ryniers F, Stove C, Goethals M, Brackenier L, Noe V, Bracke M, Vandekerckhove J, Mareel M, Bruyneel E (2002) Plasmin produces an E-cadherin fragment that stimulates cancer cell invasion. Biol Chem 383:159–165
33. Bryant DM, Kerr MC, Hammond LA, Joseph SR, Mostov KE, Teasdale RD, Stow JL (2007) EGF induces macropinocytosis and SNX1-modulated recycling of E-cadherin. J Cell Sci 120:1818–1828
34. Joslin EJ, Opresko LK, Wells A, Wiley HS, Lauffenburger DA (2007) EGF-receptor-mediated mammary epithelial cell migration is driven by sustained ERK signaling from autocrine stimulation. J Cell Sci 120:3688–3699. doi:10.1242/jcs.010488
35. Chetty R, Serra S (2008) Membrane loss and aberrant nuclear localization of E-cadherin are consistent features of solid pseudopapillary tumour of the pancreas. An immunohistochemical

study using two antibodies recognizing different domains of the E-cadherin molecule. Histopathology 52:325–330
36. Wild-Bode C, Fellerer K, Kugler J, Haass C, Capell A (2006) A basolateral sorting signal directs ADAM10 to adherens junctions and is required for its function in cell migration. J Biol Chem 281:23824–23829. doi:10.1074/jbc.M601542200
37. Kidd S, Spaeth E, Klopp A, Andreeff M, Hall B, Marini FC (2008) The (in) auspicious role of mesenchymal stromal cells in cancer: be it friend or foe. Cytotherapy 10:657–667
38. Dittmer A, Dittmer J (2006) Beta-actin is not a reliable loading control in Western blot analysis. Electrophoresis 27:2844–2845